# Photosensitized Heterogeneous Chemistry of Ozone on Organic Films

**Adla Jammoul, Saso Gligorovski,† Christian George, and Barbara D'Anna***

*Université de Lyon 1, Lyon; CNRS, UMR5256, IRCELYON, Institut de Recherches sur la Catalyse et l'Environnement de Lyon, Villeurbanne, F-69626, France*

*Received: June 5, 2007; In Final Form: November 15, 2007*

The interactions of ozone with benzophenone and phenol solid films have been investigated under simulated atmospheric conditions with respect to relative humidity, pressure, temperature, and $O_3$ concentration using a coated flow tube reactor. The steady-state reactive uptake coefficients ($\gamma_{ss}$) of ozone on benzophenone films ranged from below $10^{-6}$ in dark conditions to $\sim 4 \times 10^{-6}$ under UV-A irradiation and decreased with increasing $O_3$ concentration in the range 28−320 ppbv. A similar trend was observed for the initial uptake coefficient ($\gamma_i$) which varied from ca. $1.5 \times 10^{-6}$ in the dark to $\sim 7 \times 10^{-6}$ under UV-A irradiation. The uptake coefficients under irradiation were strongly dependent on the relative humidity (from 5 to 70%), with their lowest values at high humidity (70% RH). The ozone uptakes for multilayer coverage turned out to be independent of the deposited mass of the organic compound. The benzophenone−phenol mixture also showed photoenhanced uptake with a larger steady-state uptake under visible irradiation, $\sim 2.9 \times 10^{-6}$. Contact angle measurements showed an increase of the organic film hydrophobicity for the benzophenone−phenol mixture upon combined exposure to light and ozone. A linear dependence of the kinetic values on the photon flux has been demonstrated and when extrapolated to the solar spectral irradiance would lead to uptake coefficients of $\sim 10^{-5}$. UV−vis analysis and contact angle measurements of the organic film after irradiation and ozone exposure showed relevant changes only in the mixture, with an increase in the hydrophobic character of the film and the appearance of a new absorption band up to 450 nm.

## Introduction

Atmospheric aerosols have a major impact on the earth's climate through direct and indirect radiative forcing. They can modify cloud albedo by increasing the number of cloud droplets (Twomey effect), and they can impact cloud dynamics through changing the cloud energy balance (semidirect effect) and, consecutively, its radiative properties.[1] Organic matter accounts for a very large fraction of the tropospheric aerosol ranging from 20 to 50% of the total fine aerosol mass at continental midlatitudes and as high as 90% in tropical forested areas.[2−4]

In the troposphere, volatile organic compounds are rapidly oxidized; the resulting products are often semivolatile and tend to condense onto the preexisting particles or can eventually initiate some nucleation events. Large fractions of organic material with molecular weight between 400 and 1000 Da have been detected both in urban atmosphere and in controlled laboratory experiments.[5−13] The analysis of the water-soluble fraction of HULIS (humic-like substances) showed molecular weight up to 700 Da and concentrations of 0.2−2 $\mu g/m^3$, corresponding to 8−45% of the total organic carbon in an urban background site.[10,13] High molecular weight material can also be produced by combustion processes, like biomass burning or fossil fuel combustion.[14−19] During oxidative aging of the aerosol particles, initially nonabsorbing species can be converted into compounds that absorb both UV and visible light.[20,21] In laboratory studies, this has been shown for hydroxy-substituted aromatic compounds, typically associated with biomass burning aerosol.[20,22]

The presence of light-absorbing material can promote photosensitized processes. A photosensitizer is a compound that absorbs light and can transfer the excitation energy (from its triplet state) to another compound that hardly absorbs the available radiative energy.[23−30] Depending on the redox properties of the reaction partners and the medium, charge or energy transfer can occur to another molecule. This activates a chain reaction until transfer to, e.g., a final electron acceptor occurs.[23−25,27−32]

Despite the existence of a significant body of literature on photoinduced charge or/and energy transfer in organic molecules related to biochemistry[24,26,30,33] or to the degradation of dissolved organic matter in aquatic chemistry,[34−39]only a little is known about photochemistry of atmospheric particles and organic solid films. Nevertheless, in view of the presence of light-absorbing organic material in atmospheric particles, it should be assumed that such processes will significantly affect the aerosols chemical and physical properties during aging. For example, light-induced processes have been suggested to accelerate aging of organic particles derived from the oxidation of aliphatic hydrocarbons[40,41] and change the optical properties for aliphatic carbonyls mixed with sulfuric acid.[42] Recent composition analyses of urban surfaces such as buildings and windows show the presence of thin films of organic and inorganic material;[43] photosensitized or photoenhanced heterogeneous reactions could also occur on urban surfaces and might be able to potentially affect urban air quality. Indeed, recent papers showed that photoactivated $NO_2$ uptake onto various organic films leads to the formation of radical precursors as HONO.[44−46]

The present paper examines the interaction of ozone with some organic films under simulated atmospheric conditions. The chosen compounds are phenol and benzophenone (the sensitizer)

* Corresponding author. E-mail: barbara.danna@ircelyon.univ-lyon1.fr.
†Present address: Laboratoire de Chimie et Environnement, Université de Provence, Marseilles, France.

10.1021/jp074348t CCC: $40.75 
Published on Web 01/19/2008

since their photochemistry is well-known,[23−25,27,29,31,32] and they can be viewed as model compounds for different classes of aromatic species present in tropospheric particles.[47,48] Ozone was chosen since it is an important atmospheric trace gas and a selective oxidant. It reacts with unsaturated organic compounds, with one-electron donors such as phenoxide ions[37] and with certain radicals ($HO_2$, $NO_2$, Cl, Br). In solution, ozone can be reduced to ozonide radical ($O_3^{\bullet-}$) which decomposes readily, leading to hydroxyl radical.[37,38,49]

Heterogeneous oxidation of organic compounds by ozone under dark conditions has recently received some attention. Kinetic values and reaction products from heterogeneous ozonolysis of various organic compounds are available.[50−62] For PAHs, the heterogeneous reactivity toward ozone has been shown to be faster than the gas-phase oxidation and to be highly dependent on the substrate and degree of dispersion of the aromatic compound.[62−64] However, the effect of solar irradiation on the reactive uptake of gas traces onto organic compounds has so far been neglected. Only few studies looked at the photolysis rate of PAHs adsorbed onto solid supports and soot particles in the presence of light[65−68] and at the ice−air interface.[69]

The current paper presents a detailed kinetic study of solid films of phenol, benzophenone, and their mixture with ozone under UV−vis irradiation. The effects of ozone concentration, organic mass, irradiation type and intensity, and relative humidity have also been investigated. As well, the physicochemical properties of the films have been investigated using contact angle measurements and UV−vis spectroscopy. The potential reaction mechanisms will be briefly discussed.

## Experimental Setup

**Uptake Coefficients.** The ozone uptake coefficients onto various organic films were determined by using a coated wall flow-tube system.[70−72] A thin layer of organics was deposited in the inner section of a Pyrex tube (inner radius = 0.55 cm, length 20 cm, surface = 69 $cm^2$, and surface-to-volume ratio = 3.6 $cm^{-1}$) inserted into a larger horizontal cell maintained at constant temperature (±1 K) using a circulating water bath through the outer jacket (Huber CC 405). The humidity and the temperature of the gas flows were measured by means of a SP UFT75 sensor (Partners BV). The experiments were performed at atmospheric pressure, in a range of relative humidity (RH) between 5 and 70% and at temperatures in the range 282−288 K to prevent the evaporation of phenol (the vapor pressures at 298 K are 47 Pa for phenol and 0.1 Pa for benzophenone). The gas flows (synthetic air, $O_3$, and $N_2$ for dilution) were controlled by mass flow controllers. In the coated flow-tube the flow rate was 170−180 mL/min, ensuring a laminar regime (Reynolds's number < 100). Ozone was introduced inside the Pyrex tube through a movable injector of radius 0.3 cm and detected at the exit of the flow tube using a THERMO 49C ozone analyzer (optical detection at 252 nm). The flow tube was surrounded by seven fluorescent tubes. The latter are either visible a Phillips TLD15W/54 in the range 390−700 nm or a UV Black-Light-Blue OSRAM Sylvania TLD15W/08 in the range 340−420 nm with $\lambda_{max}$ = 365 nm. The spectral irradiance $E(\lambda)$ reaching the inner surface of the cell was quantified using two methods. The first method is based on direct measurement of the spectral irradiance using a calibrated radiometer (VLX-3W) in the range 355−375 nm. This measure is then used to scale the full spectral range of the lamps, recorded by means of an optical fiber coupled to a SR-303i Shamrock spectrograph and a fast-kinetics CCD camera (Andor Technology). The second method is based on the direct comparison of the UV-A lamps spectral irradiance with a calibrated deuterium lamp (DH-2000 Ocean Optics) using again an optical fiber. The two methods were in agreement within a factor 1.5. The irradiance in the visible spectral range has been quantified by using the UV-A data and the calibrated deuterium lamp; the two methods agreed within a factor 1.2. The spectral irradiance for the two different sets of lamps is shown in Figure 1 together with a typical solar spectral irradiance at the earth's surface (standard spectral irradiance for solar zenith of 48°).[73]

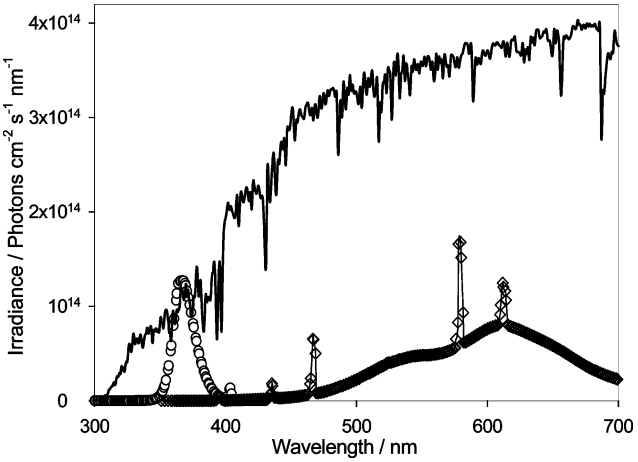


**Figure 1.** Spectral irradiance of the different light sources used in the present study. Empty circles: UV-A lamps with total irradiance in the 340−420 nm range of 2.6 × $10^{15}$ photons $cm^{-2}$ $s^{-1}$. Filled circles: visible lamps with total irradiance in the 390−700 nm range of 1.0 × $10^{16}$ photons $cm^{-2}$ $s^{-1}$. The solid line is a typical solar spectral irradiance for solar zenith of 48° clear sky derived from the standard spectrum of the American Society for Testing and Materials (ASTM), which is tilted 37° tilted toward the sun (~1.14 × $10^{17}$ photons $cm^{-2}$ $s^{-1}$ in the range 300−700 nm).

In the flow tube, the trace gas loss ($O_3$) is measured as a function of the position of the movable injector, i.e., as a function of the gas/solid exposure time. Each experimental data point, corresponding to a single position of the movable injector, is obtained on a fresh sample (newly coated tube). The linear fit of the measured ozone concentrations at four exposure times, corresponding to four different positions of the injector inside the coated flow tube, was used to derive an apparent pseudo-first-order coefficient ($k$) for the ozone decay

$$(1 - \Delta n/n) = \exp(-kt) \qquad \text{(I)}$$

where $n$ is the ozone concentration at the flow tube entrance, $\Delta n$ is the ozone consumed, and $t$ is the residence time. The raw data points from independent experiments were analyzed jointly using a weighted least-squares procedure allowing a zero-point offset.[74]

The whole process depends on several steps such as adsorption/desorption and chemical reaction of ozone at the surface sites. The total quoted uncertainties take therefore into account a combination of estimated errors for the different variables and can be expressed as

$$\left[\left(\frac{\Delta F_{O_3}}{F_{O_3}}\right)^2 + \left(\frac{\Delta F_T}{F_T}\right) + \left(\frac{\Delta T}{T}\right)^2 + \left(\frac{\Delta R}{R}\right)^2 + \left(\frac{\Delta \text{slope}}{\text{slope}}\right)^2\right]^{1/2}$$

where $F_{O_3}$ and $F_T$ are the ozone and total flow rates (STP), $T$ is the temperature in kelvin, $R$ is the inner tube radius, and slope is the pseudo-first-order coefficient. Reasonable estimates for the variables precision are $\Delta T/T = 0.01$, $\Delta F_{O_3}/F_{O_3} = 0.06$, $\Delta F_T/$

$F_T = 0.03$, $\Delta R/R = 0.10$, and an average $\Delta$slope/slope $= 0.02$. The total uncertainty is ~15%. The derived pseudo-first-order coefficient is related to the uptake coefficient ($\gamma$) though the following equation:

$$k = \gamma\langle c\rangle/2r \qquad \text{(II)}$$

where $r$ is the radius and $\langle c\rangle$ is the ozone mean thermal velocity $(8RT/\pi M)^{0.5}$.

Equation I is not valid if gas-phase diffusion limitations exist, i.e., when a radial gas concentration profile builds up. An ozone radial gradient can build up if chemical reaction at the surface is faster than gas diffusion from the center of the flow tube to the organic surface. The diffusion coefficient for $O_3$ in $N_2$ (the dilution gas in the flow tube) was calculated using the Fuller equation;[75−77] for ambient pressure and temperatures between 282 and 288 K the calculated ozone diffusion coefficient ranged between 0.125 and 0.129 $cm^2/s$, which is in good agreement with the ozone diffusion coefficient in air (ranging from 0.130 to 0.1444 $cm^2/s$) by Massman.[78] The diffusion limitation due to the ozone gradient inside the flow tube has been taken into account, and the experimental values have been corrected using the Cooney−Kim−Davis (CKD) method.[79−81] Under the experimental conditions, the correction was negligible for uptake coefficients below $\leq 2 \times 10^{-6}$ (less than 5% of the experimental value), and it increased progressively with increasing uptake coefficient to a maximum of a 20% correction for uptake coefficients of $7 \times 10^{-6}$. All the experimental data presented in the paper have been corrected for diffusion limitation.

The uptake coefficients have been evaluated after 4−5 min of exposure to ozone, the so-called initial uptake coefficient ($\gamma_i$), and after ~20 min, when the gas concentration profile reached a plateau, so-called steady-state uptake coefficient ($\gamma_{ss}$). The kinetic experiments were performed with 28−320 ppbv of ozone, 1.3−263 $\mu g/cm^2$ of organic compound, at temperatures of 285 ± 3 K and at ambient pressure.

**Contact Angle Measurements and UV−vis Spectra.** The wettability of the organic surface was probed before and after exposure to ozone and light via contact angle measurements. The contact angle is defined geometrically as the angle formed by a liquid at the three phase boundary where a liquid, a gas, and a solid intersect. After water deposition (5 $\mu$L Nanopure droplets) on the organic film the contact angle was estimated using a computer-controlled goniometric system (Digidrop GBX). The shape of the water droplet depends on the strength and the type of the interaction with the surface: a flat water droplet implies the occurrence of attractive forces with a hydrophilic substrate, while a more spherical droplet indicates the presence of repulsive forces with a hydrophilic substrate.

The experimental setup was simultaneously used to process the films for the contact angle measurements and to follow their UV−vis spectra during the photooxidative aging. The system consisted of a cylindrical Teflon reactor (20 cm length and 5 cm diameter) closed at the extremities by two Pyrex windows and aligned to a xenon lamp (75 W, Oriel) and a SR-303i Shamrock spectrograph with a fast-kinetics CCD camera (Andor Technology). The total irradiance of the xenon lamp between 300 and 700 nm was $\sim 1.8 \times 10^{17}$ photons $cm^{-2}$ $s^{-1}$ and has been evaluated as described above using a calibrated radiometer in the range 357−373 nm. The organic film was deposited on a Pyrex window, exposed to a controlled amount of ozone (100−200 ppbv) and irradiation at different exposure times.

Prior to use, the Pyrex tubes and windows were cleaned with a solution of sodium hydroxide (1 M), distilled water, then a sulfuric acid solution (0.5 M), and again with water. The organic coating was prepared using 0.5 mL of a $10^{-3}$ mol/L solution of organic species in methanol or acetone. The solvent was completely evaporated at ambient temperature by gently blowing air or $N_2$ over the film for 10−15 min.

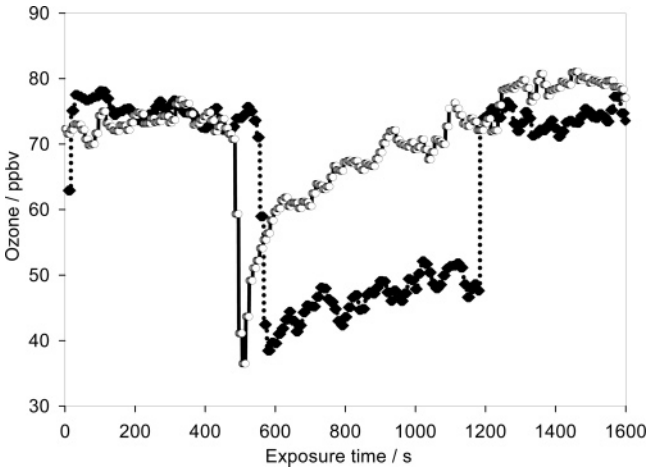


**Figure 2.** Raw data of ozone profile on a benzophenone film (2.6 $\mu g/cm^2$) exposed to 75 ppbv of ozone in dry conditions (5% RH). Empty circles: ozone profile in a dark condition experiment with visible passivation of the film; filled diamonds: irradiated experiment with UV-A ($2.7 \times 10^{15}$ photons $cm^{-2}$ $s^{-1}$) with weak time dependence of the uptake.

Benzophenone (Aldrich, 99%), phenol (Aldrich, 99%), methanol (SDS, 99.8%), sulfuric acid (Sigma-Aldrich, 95−98%), sodium hydroxide solution 32% (Riedel-de Haën) were used without any further purification.

## Results and Discussion

**Kinetics on Pure Benzophenone.** The interaction of ozone with a benzopheone solid film was investigated by means of the coated flow tube apparatus. Figure 2 shows two ozone profiles on a benzophenone film (2.6 $\mu g/cm^2$) exposed to 75 ppbv of ozone under fairly dry conditions (≤5% RH). The empty circles show a dark experiment where an initially large uptake of ozone decreases over time to an almost constant nonzero value ($\gamma_{ss}$). Steady-state ozone consumption on the surface sites is attained after 20−30 min of exposure, which is in agreement with previous studies of ozone uptake onto PAHs.[58] The second profile, filled diamonds in Figure 2, displays the ozone uptake on the benzophenone film under UV-A irradiation (total spectral irradiance of $2.7 \times 10^{15}$ photons $cm^{-2}$ $s^{-1}$ in the spectral range 340−420 nm). This profile shows a larger and irreversible uptake and a weak dependence on time; such behavior is encountered when sufficiently low ozone concentration is used and/or the reactive uptake mechanism is efficient, and the surface is not manifestly modified by the interaction over the period of exposure and/or the reaction products also show a high reactivity toward the gas trace. Figure 2 depicts two distinct reaction regimes on the same type of film and clearly demonstrates the photoenhanced ozone uptake onto the solid film.

The kinetic values were determined from the net removal of ozone in the flow tube as a function of the injector position. Each experimental data point was obtained on a fresh sample (newly coated tube). The photochemical nature of the reaction is also demonstrated in Figure 3 where the logarithmic ratio of the ozone signal is shown as a function of the residence time (determined from the flow velocity). The observed first-order loss rate was determined from the slope using eq I. The experiments were performed at 285 ± 3 K, ~5% RH, 66 ± 5

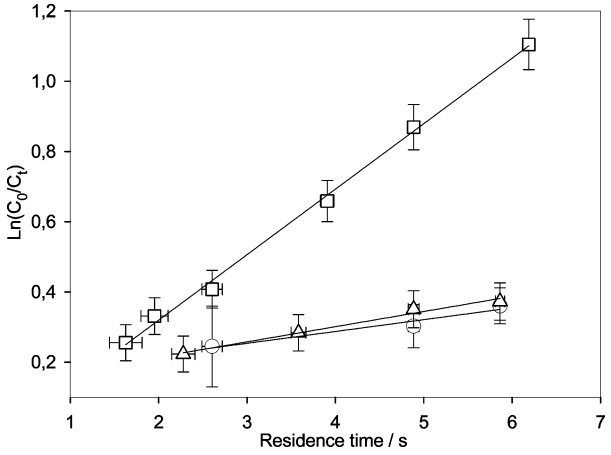


**Figure 3.** Kinetics of $O_3$ consumption (logarithmic) as a function of the residence time on a benzophenone film (2.6 $\mu$g/cm$^2$). The experimental conditions are as follow: reaction time 20 min, relative humidity 5−7%, temperature 285 ± 3 K, and ozone mixing ratio 66 ppbv. The empty triangles, squares, and circles correspond respectively to the uptake in the visible (spectral irradiance of $1.2 \times 10^{16}$ photons cm$^{-2}$ s$^{-1}$), in the UV-A (spectral irradiance of $2.7 \times 10^{15}$ photons cm$^{-2}$ s$^{-1}$) and in the dark conditions.

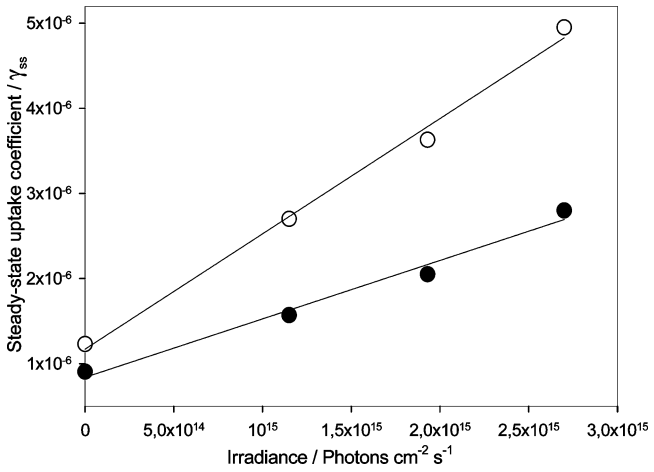


**Figure 4.** Dependence of the steady-state uptake of a benzophenone film under dry condition (5−7% RH) on the UV-A lamps irradiance in the spectral range 340-420 nm expressed as a number of photons cm$^{-2}$ s$^{-1}$ and ozone mixing ratio: 72 ppbv (filled circles) and 30 ppbv (empty circles).

ppbv of ozone. The measured steady-state uptake coefficients ($\gamma_{ss}$) were $9.8 \times 10^{-7}$ in the dark (empty circles) and $3.5 \times 10^{-6}$ under UV-A irradiation (filled diamonds). For the initial uptake coefficients ($\gamma_i$) the corresponding values were $1.5 \times 10^{-6}$ and $5.5 \times 10^{-6}$, respectively.

All the uptake coefficients obtained during the irradiated experiments represent a lower limit value to that expected in the atmosphere since under atmospheric conditions the irradiance is ∼6 times larger in the 300−400 nm range (∼$1.5 \times 10^{16}$ photons cm$^{-2}$ s$^{-1}$) and 11 times larger in the 400−700 nm range (∼$1.0 \times 10^{17}$ photons cm$^{-2}$ s$^{-1}$) using the solar spectral distribution at the earth's surface (standard spectral irradiance for solar zenith of 48°).[82] As shown in Figure 4, the uptake coefficients are linearly dependent on the UV-A spectral irradiance (from 0 to $2.7 \times 10^{15}$ photons cm$^{-2}$ s$^{-1}$ in the range 340−420 nm). If this linearity is extrapolated to the solar spectral irradiance between 340 and 420 nm at the earth's surface,[73] the derived steady-state uptake coefficients would be ∼$1.7 \times 10^{-5}$ and ∼$3 \times 10^{-5}$ for 72 and 30 ppbv ozone, respectively.

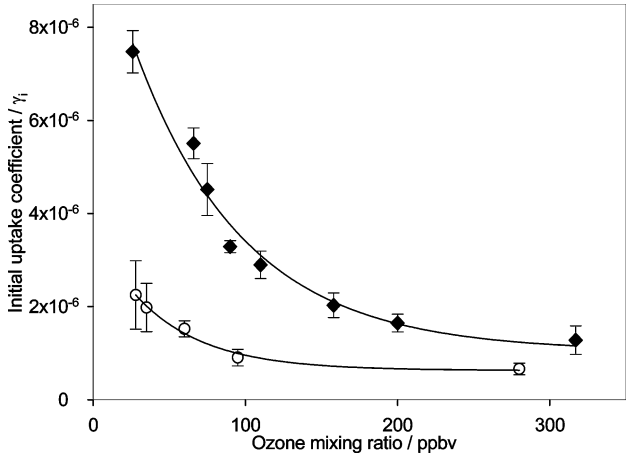


**Figure 5.** Dependence of the initial uptake coefficients of a benzophenone film (2.6 $\mu$g/cm$^2$) on the ozone mixing ratio and the light conditions. The experimental conditions are as follows: reaction time 4−5 min, relative humidity 5%, and temperature 285 ± 3 K. The filled diamonds represent the UV-A experiments (spectral irradiance $2.6 \times 10^{15}$ photons cm$^{-2}$ s$^{-1}$ in the 340−420 nm range); the empty circles represent the dark experiments.

**TABLE 1: Initial ($\gamma_i$) and Steady-State ($\gamma_{ss}$) Uptake Coefficients and Corresponding Pseudo-First-Order Rate Coefficients for a Film of Benzophenone (2.6 $\mu$g/cm$^2$) under UV-A Irradiation Corresponding to a Total Irradiance of $2.7 \times 10^{15}$ Photons cm$^{-2}$ s$^{-1}$**

| [$O_3$]/ppbv | $k_i$/s$^{-1}$ | $\gamma_i \times 10^{-6}$ | $k_{ss}$/s$^{-1}$ | $\gamma_{ss} \times 10^{-6}$ |
|---|---|---|---|---|
| 28 | 0.190 | 7.1 | 0.124 | 4.3 |
| 66 | 0.170 | 5.5 | 0.106 | 3.5 |
| 90 | 0.107 | 3.6 | 0.063 | 2.1 |
| 200 | 0.055 | 1.7 | 0.042 | 1.3 |
| 320 | 0.043 | 1.4 | 0.032 | 1.1 |

The reactive uptake onto the benzophenone film (2.6 $\mu$g/cm$^2$) under fairly dry conditions (≤5% RH) showed a strong dependence on the ozone concentration; this is demonstrated in both Figures 4 and 5. The latter illustrates that the initial uptake coefficient ($\gamma_i$) decreases from $7.1 \times 10^{-6}$ at 28 ppbv to $1.4 \times 10^{-6}$ at 320 ppbv ozone for the UV-A experiment (filled diamonds). A similar trend is also observed during the dark experiments (empty circles). The dependence on the ozone concentration suggests that the reaction proceeds via a typical Langmuir−Hinshelwood mechanism, where the reactivity occur between adsorbed species at the film surface and when all surface sites are occupied the reaction rate becomes independent of the gas concentration. This type of mechanism has been observed in many previous heterogeneous studies onto different solid and liquid organic surfaces.[51,55−57,59,83,84]

During processing the surface composition can be modified, affecting the nature of the adsorption sites and any subsequent reaction. Therefore, both chemical changes and saturation of the surface sites could explain the time dependence of the uptake coefficients, which decrease approximately 30−40% during the first 20−30 min of exposure and then stabilize. The initial ($\gamma_i$) and the steady-state ($\gamma_{ss}$) uptakes are compared in Table 1, together with the corresponding pseudo-first-order coefficients. Consumption of the reactive sites by chemical reaction and formation of nonvolatile, nonliquid, and more viscous surface products can hinder any subsequent reaction of the inner layers. This hypothesis has been invoked in previous works to explain the difference in rate constants for ozone degradation on dispersed and aggregated PAHs deposited on silica plates: indeed, for less than monolayer coverage the reaction rates were faster than for multilayer coverage.[62,63] This hypothesis can

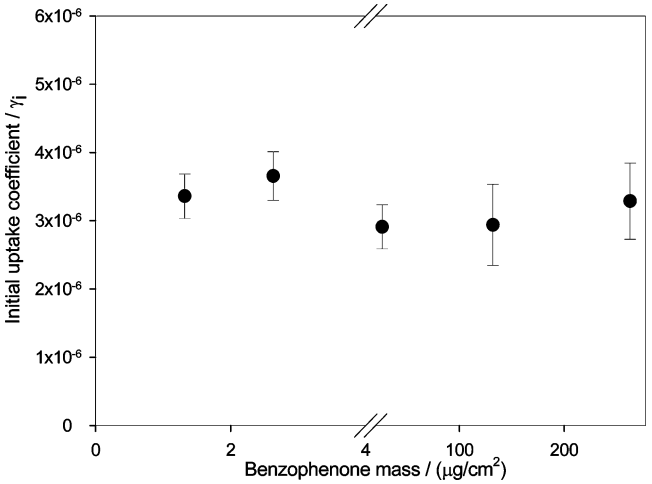


**Figure 6.** Ozone initial uptake coefficients on a benzophenone film as a function of the deposited benzophenone mass (from 1.6 to 263 $\mu$g/cm$^2$). The experiments are performed under UV-A irradiation (spectral irradiance $2.6 \times 10^{15}$ photons cm$^{-2}$ s$^{-1}$ in the 340−420 nm range), and the conditions are as follows: reaction time 4–5 min, relative humidity 5%, temperature 285 ± 3 K, and 90 ppbv of ozone.

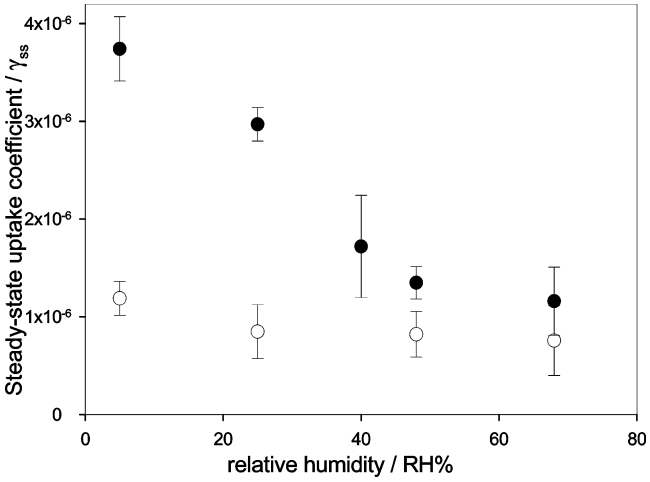


**Figure 7.** Ozone uptake coefficients on a benzophenone film (2.6 $\mu$g/cm$^2$) as a function of the relative humidity (from 5 to 70%) at 70 ppbv of ozone mixing ratio. The full and open circles correspond to the uptake coefficients in UV-A and dark conditions, respectively.

explain the features observed in Figure 6, which shows the initial uptake coefficients ($\gamma_i$) of 90 ppbv ozone with respect to the deposited mass of benzophenone (corresponding always to multilayer coverage). Indeed, constant uptakes, of $\sim 3 \times 10^{-6}$, are obtained for a large range of the organic concentrations (1.3−263 $\mu$g/cm$^2$). A similar trend is observed for the steady-state uptake coefficient. The independence of the ozone uptake with respect to the mass deposited suggests that the internal portion of the organic film does not participate in the reaction due to surface rearrangement of the nonvolatile oxidized species.[62]

As this study focuses on the uptake rates, without analysis of the products, it is difficult to assess which reactions are effectively enhanced under irradiation. It is well-known that the benzophenone triplet state is efficiently deactivated by oxygen through energy transfer with formation of both $O_2(^1\Delta_g)$ and $O_2(^1\Sigma_g^+)$,[85−89] while no charge transfer (CT) is feasible.[90] The stability of the benzophenone film with respect to singlet oxygen was tested by exposing the film to the UV light in presence of air (1 h), followed by exposure to UV light and ozone; the film showed initial and steady-state uptakes of the same order of magnitude as those observed on a fresh film directly exposed to ozone and irradiation. This provides strong evidence that singlet oxygen does not react with the film. Primary loss of $O_2(^1\Sigma_g^+)$ is believed to be via electronic quenching to $O_2(^1\Delta_g)$ by other atmospheric gases (in the atmosphere up to 10 km height the main removal process is via quenching with water vapor).[91−94] The second singlet oxygen, $O_2(^1\Delta_g)$, is also deactivated by quenching with gas-phase molecules.[91] However, in the flow tube the situation is slightly different; indeed, the two form of singlet oxygen should be formed at the film surface by energy transfer from the benzophenone triplet state and should be deactivated by gas molecules close to or adsorbed on the film. To our knowledge, adsorption parameters for ozone and water, the most important molecules in $O_2(^1\Sigma_g^+)$ quenching, at the benzophenone surface are not available. The Langmuir equilibrium constants for ozone, $K_{O_3} \approx 10^{-13}$−$10^{-15}$,[53,54,59] and for water, $K_{H_2O} \approx 10^{-17}$,[59] on a benzo[*a*]pyrene and anthracene film have therefore been used. Since the adsorption of ozone at the organic surface is enhanced with respect to that of water, deactivation of $O_2(^1\Sigma_g^+)$ by reaction with ozone has to be taken into account. The reaction products are $O_2(^1\Delta_g) + O_3$ and $2O_2 + O(^3P)$, with a yield of $O(^3P)$ between 0.75 and 1.[91,92] Under the experimental conditions, $O_2(^1\Delta_g)$ can also be quenched nonreactively by the benzophenone film,[87] while $O(^3P)$ can further react with ozone, recombine with oxygen forming ozone, and potentially react with the organic film. Its triplet state can also undergo energy transfer with ozone[95] while the reduction potentials in solution suggest that electron transfer with ozone is not possible.[96] Once formed, excited ozone is expected to be deactivated by quenching with gas-phase molecules.[97,98] Therefore, the photoenhanced ozone uptake on the solid film may be explained by a photosensitized energy transfer from the benzophenone triplet state to molecular oxygen then further reaction of the resulting $O_2(^1\Sigma_g^+)$ with ozone.

In light of the reaction mechanisms discussed above, it is possible to explain the effect of the relative humidity on the ozone uptake onto a benzophenone film. In Figure 7, the steady-state ozone uptake is presented as a function of the humidity (5−70% RH) at 70 ppbv of ozone. In dry conditions (≤5% RH) the steady-state uptake, $\sim 3.1 \times 10^{-6}$ under UV-A irradiation, is significantly higher than in the dark experiment, $\sim 1.1 \times 10^{-6}$. As humidity increases, the uptake under irradiation drops and reaches a value of $\sim 1 \times 10^{-6}$. The decrease of the ozone uptake coefficient under dark conditions as a function of the relative humidity has been reported in past studies of PAHs.[59,83] At high humidity (70%) we observe the reactive uptake of benzophenone to be reduced by 30%, which is comparable to the behavior observed by Amman, Poeschl, and co-workers.[59,83] A common interpretation is based on the competition of ozone and vapor pressure for the available reactive sites at the surface film. In the irradiated experiments the influence of humidity is more dramatic, and at high humidity (70% RH) the uptake coefficient dropped to approximately a fourth of its dry value. This additional decrease of the uptake could be explained by two separate phenomena: the competition between water and ozone in deactivating $O_2(^1\Sigma_g^+)$ at the film surface and a blue shift of the benzophenone absorption band due to the interaction with water vapor. Indeed, increasing the amount of water vapor may reduce the amount of ozone at the film surface and therefore would reduce the possibility of its removal by reaction with $O_2(^1\Sigma_g^+)$. Additionally, the carbonyl lone pair can interact with adsorbed water molecules by forming hydrogen bonds with a consequent lowering of its orbital energy, while the $\pi^*$ orbital is less affected. UV spectra of benzophe-

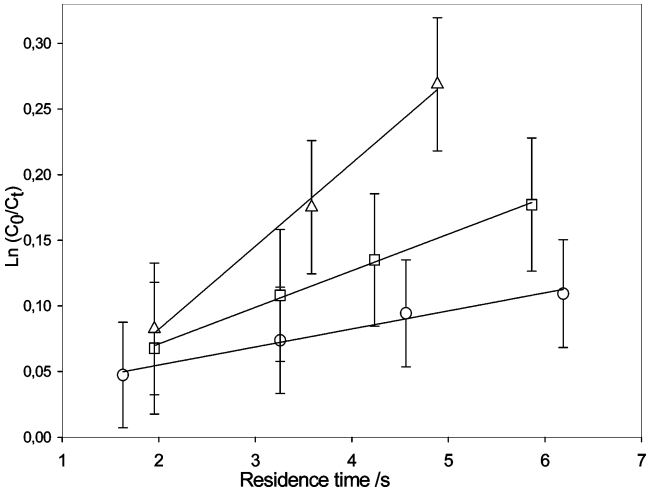


**Figure 8.** Kinetics of $O_3$ consumption (logarithmic) as a function of the residence time on a benzophenone−phenol mixture (1:1 and mass deposited). The experimental conditions are as follows: reaction time 20 min, relative humidity 5%, temperature 285 ± 3 K, and ozone mixing ratio 60 ppbv. The empty triangles, squares, and circles correspond to the uptake in the visible (spectral irradiance of $1.2 \times 10^{16}$ photons $cm^{-2}$ $s^{-1}$), in the UV-A (spectral irradiance of $2.7 \times 10^{15}$ photons $cm^{-2}$ $s^{-1}$) and under dark conditions, respectively.

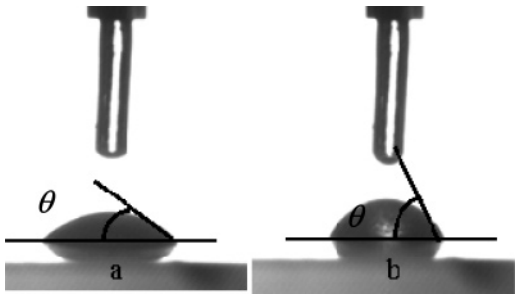


**Figure 9.** Pictures of two 0.5 μL water droplets deposited on the benzophenone−phenol film (0.18 mg/cm$^2$) before (a) and after (b) exposure for 120 min to 200 ppbv of ozone and irradiation with a xenon lamps (the total number of photons $cm^{-2}$ $s^{-1}$ in the 300−400 nm range is $5.6 \times 10^{15}$ and in the 400−700 nm range is $1.7 \times 10^{17}$). Contact angles are marked with black lines.

none in several solvents (cyclohexane, acetonitrile, ethanol, and water) showed higher n → π* energy transition as the solvent polarity increased. The transition in water occurs at $\lambda \leq 350$ nm, reducing the overlap with the spectrum of the fluorescent lights (UV-A) used here and therefore perhaps reducing the efficiency of the photosensitized process.

**Kinetics on Benzophenone−Phenol.** Benzophenone is an efficient photosensitizer able to initiate reactions with nonabsorbing organic species by hydrogen or charge transfer.[23−25,27−32] We therefore investigated the ozone uptake on a (1:1) mixture of benzophenone and phenol in order to recognize the role of a photosensitizer (benzophenone) with respect to a nonabsorbing species (phenol). No photoenhanced ozone uptake was observed on a pure phenol film, which is consistent with the absence of any absorption features in the spectral region of the lamps (both UV and visible), while photoenhanced uptake was observed on the mixed film when irradiated (Figure 8). The experiments were performed at 285 ± 3 K, 5−7% RH, 80 ± 5 ppbv of $O_3$. The measured steady-state uptake coefficients ($\gamma_{ss}$) obtained from the pseudo-fist-order loss rate were $6.7 \times 10^{-7}$ in the dark (empty circles), $1.1 \times 10^{-6}$ under UV-A irradiation (empty squares), and $2.9 \times 10^{-6}$ under visible irradiation (empty triangles). A complete set of experimental kinetic values for the mixture are presented in Table 2. The mixture behaved

**TABLE 2: Initial ($\gamma_i$) and Steady-State ($\gamma_{ss}$) Uptake Coefficients and Corresponding Pseudo-First-Order Rate Coefficients for a Dry Film of Benzophenone−Phenol (2.6 μg/cm$^2$) under UV-A and Visible Irradiation**

| $[O_3]$/ppbv | irradiation | $k_i/s^{-1}$ | $\gamma_i \times 10^{-6}$ | $k_{ss}/s^{-1}$ | $\gamma_{ss} \times 10^{-6}$ |
|---|---|---|---|---|---|
| 80 | no light | 0.039 | 1.5 | 0.016 | 0.6 |
| 80 | vis | 0.120 | 4.3 | 0.050 | 2.9 |
| 80/25% RH | vis | 0.091 | 2.8 | 0.046 | 1.4 |
| 80/48% RH | vis | 0.086 | 2.6 | 0.039 | 1.2 |
| 80/70% RH | vis | 0.068 | 2.1 | 0.019 | 1.0 |
| 80 | UV | 0.064 | 2.2 | 0.032 | 1.1 |
| 45 | UV−vis | 0.100 | 3.6 | 0.069 | 2.5 |
| 56 | UV−vis | 0.090 | 3.1 | 0.060 | 2.1 |
| 80 | UV−vis | 0.078 | 2.9 | 0.047 | 1.8 |

similarly to the benzophenone film with respect to ozone mixing ratio and humidity; however, it showed larger photoenhanced uptake under visible irradiation. This intriguing feature is quite difficult to explain since neither of the two organic compounds absorbs visible light, and only ozone can absorb in this region (Chappuis band). However, the excited ozone does not affect the kinetics when the film is formed by a single component. Indeed, under visible irradiation the ozone uptake by films of phenol and benzophenone were both $\sim 1 \times 10^{-6}$, as for the dark experiments. So what can be tentatively suggested is the formation of a complex. Under UV-A irradiation two possible processes might occur: the first, already discussed, involves energy transfer from benzophenone triplet state to oxygen; the second entails interaction between the two organic species with formation of radicals which further react with ozone. The benzophenone triplet state (285 kJ/mol) is not able to undergo any energy transfer with phenol, which has a higher triplet state energy (342 kJ/mol). In solution, however, oxidation of phenol by benzophenone triplet state occurs through charge-transfer (CT) and/or hydrogen abstraction, depending on the polarity of the solvent.[24,25,30] The reaction leads to the formation of ketyl radical and phenoxy radicals.[23−25,27,28] In organic solutions, in the presence of oxygen, the ketyl radical is mainly reoxidized to ketone and $O_2^{\bullet-}/HO_2^{\bullet}$ are generated,[25] so additional reactions could take place between the organic film and the oxidants formed. The phenoxy radical is also known to react with ozone and form ozonide radical ($O_3^{\bullet-}$) followed by $O_2$ and $O^{\bullet-}$ formation, which in presence of water leads to hydroxyl radical formation.[49] In addition, the phenoxy radicals can further react with oxygen[25] or dimerize.[20,37] Such reactions can possibly occur at the surface of the film while they should be hindered in the bulk, since in solid films disproportion of the radicals with regeneration of the starting reactants becomes important. This is caused by the low molecular mobility that strongly hinders the rearrangement of species, which is necessary for the formation of radical recombination products.[28]

**Contact Angle Measurements and UV−vis Analysis.** As already mentioned above, the surface of the organic film is changing when exposed to ozone and light. The physicochemical changes were evaluated by measuring the contact angles (with respect to pure liquid water) of the film (pure benzophenone, pure phenol, and the mixture). In Table 3, the contact angle measurements for organic films before and after exposure to relatively high ozone mixing ratio (100−200 ppbv) and irradiation by the output of a 75 W xenon lamp are presented. The phenol film does not show any remarkable change upon exposure to ozone or/and light; in the table only the results relative to the ozone treatment are shown. When the benzophenone film is exposed to ozone or/and light, the contact angle shows a slight increase by 5°−8°; however, ±5° was the typical variance due the nonhomogeneity of the film surface. Therefore,

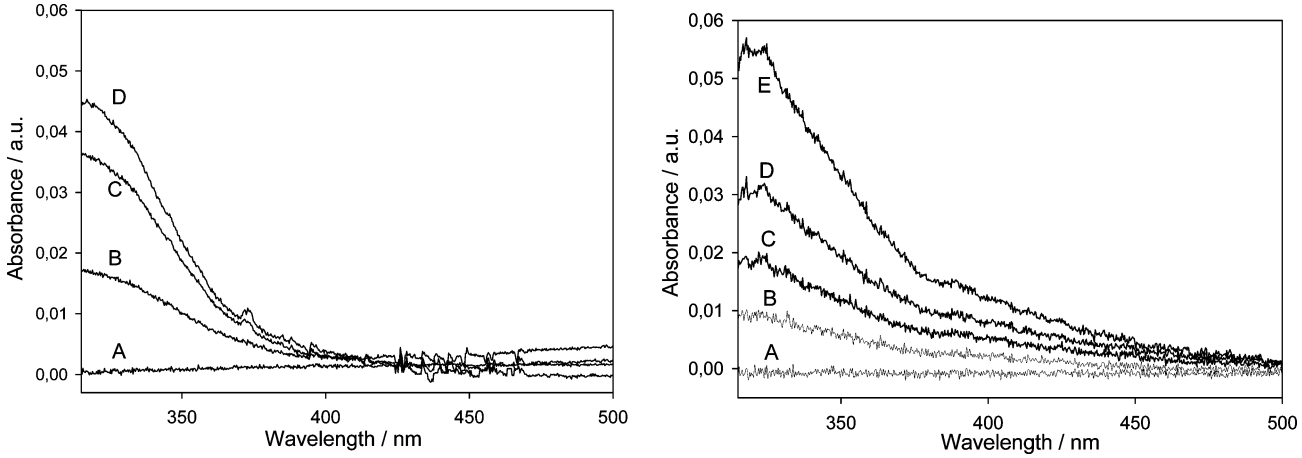


**Figure 10.** UV/vis spectra of a benzophenone−phenol film (0.18 mg/cm$^2$) exposed to 200 ppbv of ozone and to irradiation with a xenon lamps during different time. The letters A, B, C, D, and E correspond to 0, 20, 42, 73, and 120 min of exposure time, respectively.

**TABLE 3: Summary of the Contact Angle Measurements for Single Component and Mixed Organics before and after Exposure to Ozone and Irradiation of a Xenon Lamp (Total Irradiance between 300 and 700 nm 1.8 × 10$^{17}$ Photons cm$^{-2}$ s$^{-1}$)**

| | | | | contact angle (deg) | | |
|---|---|---|---|---|---|---|
| compound | amount | [$O_3$]/ppbv | exposure time/min | before | after | exposure type |
| phenol | 0.1 mg | 100 | 25 | 39 | 37 | ozone |
| benzophenone | 0.5 mg | 200 | 170 | 40 | 45 | ozone |
| benzophenone | 0.5 mg | 200 | 80 | 36 | 41 | light |
| benzophenone | 0.5 mg | 200 | 170 | 38 | 45.9 | ozone and light |
| benzophenone−phenol | 0.5 mg ratio 1:1 | 200 | 100 | 34 | 35 | light |
| benzophenone−phenol | 0.5 mg ratio 1:1 | 200 | 170 | 37 | 54.7 | ozone and light |
| benzophenone−phenol | 0.5 mg ratio 1:1 | 200 | 70 | 35 | 50.8 | ozone and light |

it is not clear whether the benzophenone film really becomes more hydrophobic. For the mixed film the situation is quite different; indeed, no changes are observed when exposed only to light or to ozone, while a relevant increase of the contact angle, approximately 15−18°, is observed when the film is exposed to both light and ozone. Figure 9 shows a 5 $\mu$L water droplet on a benzophenone−phenol film before (a) and after (b) exposure to 200 ppbv ozone and light for 70 min. Consistent with the Young equation, the contact angle of the surface becomes larger if the surface tension of the liquid is increased. Surface roughness and surface heterogeneity may also increase the contact angle due to the destabilization of the water droplet covering the surface. Despite the observation that oxidative processes are thought to convert hydrophobic coating into polar (e.g., see refs 99 and 100), the observed changes of the surface wettability have been interpreted as a possible formation of more hydrophobic products or/and reorganization of the surface layers.[62,101,102] A similar interpretation has been proposed for ozonation of PAHs[62] and self-assembled monolayers, where formation of large organic aggregates was demonstrated.[103]

Figure 10 shows the changes in the UV/vis spectral region for a pure benzophenone film (left plot) and for a benzophenone-phenol film (right plot) exposed under dry conditions (≤5% RH) to 200 ppbv of ozone and irradiation of a xenon lamp (total spectral irradiance in the 300−700 nm range of 1.7 × 10$^{17}$ photons cm$^{-2}$ s$^{-1}$) at different exposure times. The spectral reference (A) is the unreacted film at time zero when the film is inserted into the reactor. Therefore, all subsequent spectra are just changes relative to this reference and concern the appearance of new optical features. The letters B, C, D, and E correspond to increasing exposure times to light and ozone of the solid film (30, 42, 90, and 125 for the benzophenone film and 20, 42, 73, and 120 min for the mixture). The two films show some changes in the spectral features during the reaction time; for the benzophenone film a new band appeared in the UV-A region while in the mixture this band reached ∼450 nm, and the film, initially white-transparent, became yellow. The appearance of an absorption band up to 450 nm (a yellow product) is linked to the presence of conjugated compounds which can be explained, as discussed above, by the photosensitized formation of radicals (mainly phenoxy) that might undergo radical dimerization by radical coupling[20] or can react further with trace gases and oxidants.[25] Similar UV−vis spectra and colored material have been observed in previous laboratory studies where dihydroxybenzoic acid in solution was processed in presence of traces of iron and hydrogen peroxide (Fenton-type reaction).[20]

## Conclusions

The present paper demonstrated the photochemical and photosensitized nature of the ozone uptake onto benzophenone and benzophenone−phenol solid films. For low $O_3$-mixing ratios (typical for continental clean areas), dry conditions (5% RH) and UV-A irradiation the initial uptake coefficient of benzophenone was ∼7 × 10$^{-6}$ and declined to ∼1.4 × 10$^{-6}$ for very high ozone mixing ratios. The uptake coefficients showed time dependence with a decay of approximately 30−40% during the first 20−30 min of exposure. The kinetic values were independent of the deposited mass (always multilayers), suggesting that the internal portion of the organic film did not participate in the reaction. The photoenhanced ozone uptake on solid benzophenone was tentatively explained by a photosensitized energy transfer from the triplet state of benzophenone to molecular oxygen and further reaction of $O_2(^1\Sigma_g^+)$ with ozone.

Additional kinetic studies have been performed on the mixture of benzophenone with phenol; the uptakes showed similar behavior with respect to humidity and ozone mixing ratios to what was observed for the benzophenone film. The photoenhanced reactivity of ozone with the mixture under UV-A

irradiation has been tentatively explained by the photosensitized energy transfer from the triplet state of benzophenone to molecular oxygen and by charge-transfer (CT) and/or hydrogen abstraction of excited benzophenone with phenol with formation of the ketyl radical. This should mainly react with oxygen but could also react with ozone trough electron transfer. The mixture presented another intriguing feature: the organic mixture showed the highest uptake coefficient when exposed to visible irradiation, while benzophenone showed a larger uptake coefficient only when exposed to UV-A irradiation. This unexpected behavior has been tentatively explained by the formation of intermediate adducts between the organic reactants and ozone.

The uptake coefficients for the irradiated experiments should be considered as lower limit values. The spectral irradiance of the UV-A lamps was ~6 times smaller than the solar irradiance at the earth's surface and did not cover the range below 340 nm where benzophenone and other atmospheric photosensitizers are absorbing. For the visible lamps the situation was even more critical since the irradiance was 11 times smaller than the irradiance reaching the surface of the planet. Nevertheless, the present work demonstrated the linearity between ozone uptake coefficients and irradiance for the benzophenone film, and when this linearity was extrapolated to realistic solar irradiance, the uptakes reached $\sim 10^{-5}$.

Despite the limitation due to reduced light irradiance, the present paper showed that ozone uptake was photochemically enhanced on these organic films and presented a possible route for the formation of species absorbing in the visible starting from a UV-absorbing (benzophenone) and a nonabsorbing (phenol) species. It can be concluded that photoinduced processes of organic photosensitizers (as aromatic ketones) present in submicron aerosols or deposited on urban surfaces (buildings, windows) may represent a potential new route for the formation of larger and more hydrophobic organic material.

It is obvious that the present study has been conducted under highly simplified conditions, but it clearly illustrates that photoenhanced processes on atmospheric surfaces should be considered in forthcoming studies. Of course, such "clean" conditions are not present in the atmosphere. However, the light-absorbing fraction of organic aerosol is quite important and may act as atmospheric photosensitizer similarly to what has been observed on natural water containing humic or fulvic substances.[24,25] Similar processes may certainly occur with atmospheric HULIS or even (as shown here) with simpler model compounds.

**Acknowledgment.** We thank EUCAARI, Primequal-2 and Lefe-Chat, and the French Research Ministry for financial support.

## References and Notes

(1) IPCC Cambridge University Press, 2007.
(2) Andreae, M. O.; Crutzen, P. J. *Science (Washington, D.C.)* **1997**, *276*, 1052.
(3) Roberts, G. C.; Artaxo, P.; Zhou, J.; Swietlicki, E.; Andreae, M. O. *J. Geophys. Res., [Atmos.]* **2002**, *107*, LBA37/1.
(4) Talbot, R. W.; Andreae, M. O.; Andreae, T. W.; Harriss, R. C. *J. Geophys. Res., [Atmos.]* **1988**, *93*, 1499.
(5) Gelencser, A.; Hoffer, A.; Krivacsy, Z.; Kiss, G.; Molnar, A.; Meszaros, E. *J. Geophys. Res., [Atmos.]* **2002**, *107*, ICC2/1.
(6) Jang, M.; Czoschke, N. M.; Lee, S.; Kamens, R. M. *Science (Washington, D.C.*) **2002**, *298*, 814.
(7) Jang, M.; Czoschke, N. M.; Northcross, A. L. *ChemPhysChem* **2004**, *5*, 1646.
(8) Jang, M.; Lee, S.; Kamens, R. M. *Atmos. Environ.* **2003**, *37*, 2125.
(9) Kalberer, M.; Paulsen, D.; Sax, M.; Steinbacher, M.; Dommen, J.; Prevot, A. S. H.; Fisseha, R.; Weingartner, E.; Frankevich, V.; Zenobi, R.; Baltensperger, U. *Science (Washington, D.C.)* **2004**, *303*, 1659.
(10) Limbeck, A.; Handler, M.; Neuberger, B.; Klatzer, B.; Puxbaum, H. *Anal. Chem.* **2005**, *77*, 7288.
(11) Salma, I.; Ocskay, R.; Chi, X.; Maenhaut, W. *Atmos. Environ.* **2007**, *41*, 4106.
(12) Samburova, V.; Didenko, T.; Kunenkov, E.; Emmenegger, C.; Zenobi, R.; Kalberer, M. *Atmos. Environ.* **2007**, *41*, 4703.
(13) Samburova, V.; Zenobi, R.; Kalberer, M. *Atmos. Chem. Phys.* **2005**, *5*, 2163.
(14) Decesari, S.; Facchini, M. C.; Matta, E.; Mircea, M.; Fuzzi, S.; Chughtai, A. R.; Smith, D. M. *Atmos. Environ.* **2002**, *36*, 1827.
(15) Gonzalez-Perez, J. A.; Gonzalez-Vila, F. J.; Almendros, G.; Knicker, H. *Environ. Int.* **2004**, *30*, 855.
(16) Hoffer, A.; Kiss, G.; Blazso, M.; Gelencser, A. *Geophys. Res. Lett.* **2004**, *31*, L06115/1.
(17) Holmes, B. J.; Petrucci, G. A. *Environ. Sci. Technol.* **2006**, *40*, 4983.
(18) Kirchstetter, T. W.; Novakov, T.; Hobbs, P. V. *J. Geophys. Res., [Atmos.]* **2004**, *109*, D21208/1.
(19) Mayol-Bracero, O. L.; Guyon, P.; Graham, B.; Roberts, G.; Andreae, M. O.; Decesari, S.; Facchini, M. C.; Fuzzi, S.; Artaxo, P. *J. Geophys. Res., [Atmos.]* **2002**, *107*, LBA59/1.
(20) Gelencser, A.; Hoffer, A.; Kiss, G.; Tombacz, E.; Kurdi, R.; Bencze, L. *J. Atmos. Chem.* **2003**, *45*, 25.
(21) Gomez, A. L.; Park, J.; Walser, M. L.; Lin, A.; Nizkorodov, S. A. *J. Phys. Chem. A* **2006**, *110*, 3584.
(22) Krivacsy, Z.; Kiss, G.; Varga, B.; Galambos, I.; Sarvari, Z.; Gelencser, A.; Molnar, A.; Fuzzi, S.; Facchini, M. C.; Zappoli, S.; Andracchio, A.; Alsberg, T.; Hansson, H. C.; Persson, L. *Atmos. Environ.* **2000**, *34*, 4273.
(23) Becker, H. D. *J. Org. Chem.* **1967**, *37*, 2124.
(24) Canonica, S.; Hellrung, B.; Wirz, J. *J. Phys. Chem. A* **2000**, *104*, 1226.
(25) Canonica, S.; Jans, U.; Stemmler, K.; Hoigne, J. *Environ. Sci. Technol.* **1995**, *29*, 1822.
(26) Canonica, S.; Kohn, T.; Mac, M.; Real, F. J.; Wirz, J.; Von, Gunten, U. *Environ. Sci. Technol.* **2005**, *39*, 9182.
(27) Das, P. K.; Encinas, M. V.; Scaiano, J. C. *J. Am. Chem. Soc.* **1981**, *103*, 4154.
(28) Ivanov, V. B.; Kutsenova, A. V.; Khavina, E. Y. *Russ. Chem. Bull.* **2005**, *54*, 1445.
(29) Lathioor, E. C.; Leigh, W. J.; St. Pierre, M. J. *J. Am. Chem. Soc.* **1999**, *121*, 11984.
(30) Leigh, W. J.; Lathioor, E. C.; St. Pierre, M. J. *J. Am. Chem. Soc.* **1996**, *118*, 12339.
(31) Lathioor, E. C.; Leigh, W. J. *Can. J. Chem.* **2001**, *79*, 1851.
(32) Sultimova, N. B.; Levin, P. P.; Chaikovskaya, O. N.; Sokolova, I. V.; Kuzmin, A. V. *Proc. Int. Soc. Opt. Eng.* **2004**, *5396*, 178.
(33) Giese, B.; Napp, M.; Jacques, O.; Boudebous, H.; Taylor, A. M.; Wirz, J. *Angew. Chem., Int. Ed.* **2005**, *44*, 4073.
(34) Benitez, F. J.; Beltran-Heredia, J.; Acero, J. L.; Pinilla, M. L. *J. Chem. Technol. Biotechnol.* **1997**, *70*, 253.
(35) Haag, W. R.; Hoigne, J.; Gassman, E.; Braun, A. M. *Chemosphere* **1984**, *13*, 641.
(36) Huang, C.-R.; Shu, H.-Y. *J. Hazard. Mater.* **1995**, *41*, 47.
(37) Mvula, E.; von Sonntag, C. *Org. Biomol. Chem.* **2003**, *1*, 1749.
(38) Poznyak, T.; Vivero, J. *Ozone: Sci. Eng.* **2005**, *27*, 447.
(39) Wu, J. J.; Masten, S. J. *Water Res.* **2002**, *36*, 1513.
(40) Gomez, A. L.; Park, J.; Walser, M. L.; Lin, A.; Nizkorodov, S. A. *J. Phys. Chem. A* **2006**, *110*, 3584.
(41) Park, J.; Gomez, A. L.; Walser, M. L.; Lin, A.; Nizkorodov, S. A. *Phys. Chem. Chem. Phys.* **2006**, *8*, 2506.
(42) Noziere, B.; Esteve, W. *Atmos. Environ.* **2007**, *41*, 1150.
(43) Lam, B.; Diamond, M. L.; Simpson, A. J.; Makar, P. A.; Truong, J.; Hernandez-Martinez, N. A. *Atmos. Environ.* **2005**, *39*, 6578.
(44) George, C.; Strekowski, R. S.; Kleffmann, J.; Stemmler, K.; Ammann, M. *Faraday Discuss.* **2005**, *130*, 195.
(45) Stemmler, K.; Ndour, M.; Elshorbany, Y.; Kleffmann, J.; Ammann, M.; D'Anna, B.; George, C.; Bohn, B. *Atmos. Chem. Phys. Discuss.* **2007**, *7*, 4035.
(46) Stemmler, K.; Ammann, M.; Donders, C.; Kleffmann, J.; George, C. *Nature (London)* **2006**, *440*, 195.
(47) Ikarashi, Y.; Kaniwa, M.-a.; Tsuchiya, T. *Chemosphere* **2005**, *60*, 1279.
(48) Zimmermann, R.; Heger, H. J.; Blumenstock, M.; Dorfner, R.; Nikolai, U.; Schramm, K. W.; Kettrup, A. *Organohalogen Compd.* **1999**, *40*, 321.
(49) Staehelin, J.; Hoigne, J. *Environ. Sci. Technol.* **1985**, *19*, 1206.
(50) Alekseeva, O. V.; Razumovskii, S. D. *Kinet. Catal.* **2006**, *47*, 533.
(51) Dubowski, Y.; Vieceli, J.; Tobias, D. J.; Gomez, A.; Lin, A.; Nizkorodov, S. A.; McIntire, T. M.; Finlayson-Pitts, B. J. *J. Phys. Chem. A* **2004**, *108*, 10473.
(52) Kornmuller, A.; Wiesmann, U. *Water Res.* **2003**, *37*, 1023.

(53) Kwamena, N.-O. A.; Earp, M. E.; Young, C. J.; Abbatt, J. P. D. *J. Phys. Chem. A* **2006**, *110*, 3638.
(54) Kwamena, N.-O. A.; Thornton, J. A.; Abbatt, J. P. D. *J. Phys. Chem. A* **2004**, *108*, 11626.
(55) McNeill, V. F.; Wolfe, G. M.; Thornton, J. A. *J. Phys. Chem. A* **2007**, *111*, 1073.
(56) Mmereki, B. T.; Donaldson, D. J. *J. Phys. Chem. A* **2003**, *107*, 11038.
(57) Mmereki, B. T.; Donaldson, D. J.; Gilman, J. B.; Eliason, T. L.; Vaida, V. *Atmos. Environ.* **2004**, *38*, 6091.
(58) Perraudin, E.; Budzinski, H.; Villenave, E. *J. Atmos. Chem.* **2007**, *56*, 57.
(59) Poeschl, U.; Letzel, T.; Schauer, C.; Niessner, R. *J. Phys. Chem. A* **2001**, *105*, 4029.
(60) Raja, S.; Valsaraj, K. T. *J. Air Waste Manage. Assoc.* **2005**, *55*, 1345.
(61) Raja, S.; Valsaraj, K. T. *Atmos. Res.* **2006**, *81*, 277.
(62) Wu, C. H.; Salmeen, I.; Niki, H. *Environ. Sci. Technol.* **1984**, *18*, 603.
(63) Alebic-Juretic, A.; Cvitas, T.; Klasinc, L. *Environ. Sci. Technol.* **1990**, *24*, 62.
(64) Alebic-Juretic, A.; Cvitas, T.; Klasinc, L. *Chemosphere* **2000**, *41*, 667.
(65) Cope, V. W.; Kalkwarf, D. R. *Environ. Sci. Technol.* **1987**, *21*, 643.
(66) Kamens, R. M.; Guo, Z.; Fulcher, J. N.; Bell, D. A. *Environ. Sci. Technol.* **1988**, *22*, 103.
(67) Kamens, R. M.; Perry, J. M.; Saucy, D. A.; Bell, D. A.; Newton, D. L.; Brand, B. *Environ. Int.* **1985**, *11*, 131.
(68) Pitts, J. N., Jr.; Paur, H. R.; Zielinska, B.; Arey, J.; Winer, A. M.; Ramdahl, T.; Mejia, V. *Chemosphere* **1986**, *15*, 675.
(69) Kahan, T. F.; Donaldson, D. J. *J. Phys. Chem. A* **2007**, *111*, 1277.
(70) Kane, S. M.; Timonen, R. S.; Leu, M.-T. *J. Phys. Chem. A* **1999**, *103*, 9259.
(71) Percival, C. J.; Mossinger, J. C.; Anthony Cox, R. *Phys. Chem. Chem. Phys.* **1999**, *1*, 4565.
(72) Strekowski, R. S.; George, C. *J. Chem. Eng. Data* **2005**, *50*, 804.
(73) Gueymard, C. A.; Myers, D.; Emery, K. *Sol. Energy* **2002,** *73*, 443−467 (http://rredc.nrel.gov/solar/spectra/am1.5/#Gueymard2).
(74) York, D. *Can. J. Phys.* **1996**, *44*, 1079.
(75) Fuller, E. N.; Ensley, K.; Giddings, J. C. *J. Phys. Chem.* **1969**, *73*, 3679.
(76) Fuller, E. N.; Giddings, J. C. *J. Gas Chromatogr.* **1965**, *3*, 222.
(77) Fuller, E. N.; Schettler, P. D.; Giddings, J. C. *J. Ind. Eng. Chem.* **1966**, *58*, 18.
(78) Massman, W. J. *Atmos. Environ.* **1998**, *32*, 1111.
(79) Behnke, W.; George, C.; Scheer, V.; Zetzsch, C. *J. Geophys. Res., [Atmos.]* **1997**, *102*, 3795.
(80) Cooney, D. O.; Kim, S. S.; Davis, E. J. *Chem. Eng. Sci.* **1974**, *29*, 1731.
(81) Murphy, D. M.; Fahey, D. W. *Anal. Chem.* **1987**, *59*, 2753.
(82) Gueymard, C. A.; Myers, D.; Emery, K. *Sol. Energy* **2002**, *73*, 443−467 (http://rredc.nrel.gov/solar/spectra/am1.5/#Gueymard2).
(83) Ammann, M.; Poeschl, U.; Rudich, Y. *Phys. Chem. Chem. Phys.* **2003**, *5*, 351.
(84) Kahan, T. F.; Kwamena, N. O. A.; Donaldson, D. J. *Atmos. Environ.* **2006**, *40*, 3448.
(85) Bodesheim, M.; Schuetz, M.; Schmidt, R. *Chem. Phys. Lett.* **1994**, *221*, 7.
(86) Schmidt, R.; Bodesheim, M. *Chem. Phys. Lett.* **1993**, *213*, 111.
(87) Schweitzer, C.; Mehrdad, Z.; Noll, A.; Grabner, E.-W.; Schmidt, R. *Helv. Chim. Acta* **2001**, *84*, 2493.
(88) Wang, B.; Ogilby, P. R. *J. Phys. Chem.* **1993**, *97*, 9593.
(89) Wang, B.; Ogilby, P. R. *J. Photochem. Photobiol., A* **1995**, *90*, 85.
(90) Mehrdad, Z.; Noll, A.; Grabner, E.-W.; Schmidt, R. *Photochem. Photobiol. Sci.* **2002**, *1*, 263.
(91) Atkinson, R.; Baulch, D. L.; Cox, R. A.; Crowley, J. N.; Hampson, R. F.; Hynes, R. G.; Jenkin, M. E.; Rossi, M. J.; Troe, J. *Atmos. Chem. Phys.* **2004**, *4*, 1461.
(92) Dunlea, E. J.; Talukdar, R. K.; Ravishankara, A. R. *J. Phys. Chem. A* **2005**, *109*, 3912.
(93) Park, H.; Slanger, T. G. *J. Chem. Phys.* **1994**, *100*, 287.
(94) Price, J. M.; Mack, J. A.; Rogaski, C. A. A.; Wodtke, A. M. *Chem. Phys.* **1993**, *175*, 83.
(95) Ohtsuka, Y.; Hasegawa, J.-y.; Nakatsuji, H. *Chem. Phys.* **2007**, *332*, 262.
(96) Klaning, U. K.; Sehested, K.; Holcman, J. *J. Phys. Chem.* **1985**, *89*, 760.
(97) Kurylo, M. J.; Braun, W.; Kaldor, A. *Chem. Phys. Lett.* **1974**, *27*, 249.
(98) Rosen, D. I.; Cool, T. A. *J. Chem. Phys.* **1973**, *59*, 6097.
(99) Asad, A.; Mmereki, B. T.; Donaldson, D. J. *Atmos. Chem. Phys.* **2004**, *4*, 2083.
(100) Bertram, A. K.; Ivanov, A. V.; Hunter, M.; Molina, L. T.; Molina, M. J. *J. Phys. Chem. A* **2001**, *105*, 9415.
(101) Bismarck, A.; Kumru, M. E.; Springer, J. *J. Colloid Interface Sci.* **1999**, *217*, 377.
(102) McIntire, T. M.; Lea, A. S.; Gaspar, D. J.; Jaitly, N.; Dubowski, Y.; Li, Q.; Finlayson-Pitts, B. J. *Phys. Chem. Chem. Phys.* **2005**, *7*, 3605.